

**In vivo activation of human PXR tightens the blood-brain barrier to
methadone through P-glycoprotein upregulation**

**Björn Bauer, Xiaodong Yang, Anika M.S. Hartz, Emily R. Olson, Rong Zhao, J. Cory
Kalvass, Gary M. Pollack, and David S. Miller**

Laboratory of Pharmacology and Chemistry, National Institute of Environmental Health
Sciences, National Institutes of Health, Research Triangle Park, NC 27709, USA (BB, AMSH,
DSM)

Division of Drug Delivery and Disposition, School of Pharmacy, University of North Carolina,
Chapel Hill, NC 27599-7360, USA (XY, ERO, RZ, JCK, GMP)

Running Title: hPXR Activation and Methadone Efficacy

Corresponding Author: **Dr. David S. Miller**
Laboratory of Pharmacology and Chemistry
National Institute of Environmental Health Sciences
National Institutes of Health
111 TW Alexander Dr
Research Triangle Park, NC 27709

phone: 919 541 3235
fax: 919 541 5737
miller@niehs.nih.gov

31 Text pages

0 Tables

6 Figures

28 References

Abstract: 213 words

Introduction: 554 words

Discussion: 558 words

Nonstandard Abbreviations:

Dulbecco's phosphate buffered saline, DPBS; [N- ϵ (4-nitrobenzofurazan-7-yl)-D-Lys⁸]-cyclosporine A, NBD-CSA; human pregnane X receptor, hPXR; pregnane X receptor, PXR; pregnenolone 16 α -carbonitrile, PCN

ABSTRACT

The ATP-driven drug export pump, P-glycoprotein, is a primary gatekeeper of the blood-brain barrier and a major impediment to CNS pharmacotherapy. Reducing P-glycoprotein activity dramatically increases penetration of many therapeutic drugs into the CNS. Previous studies in rat demonstrated that brain capillary P-glycoprotein was transcriptionally upregulated by the pregnane X receptor (PXR), a xenobiotic-activated nuclear receptor. Here we used a transgenic mouse expressing human PXR (hPXR) to determine the consequences of increased blood-brain barrier P-glycoprotein activity. P-glycoprotein expression and transport activity in brain capillaries from transgenic mice was significantly increased when capillaries were exposed to the hPXR ligands, rifampin and hyperforin, *in vitro* and when the mice were dosed with rifampin *in vivo*. Plasma rifampin levels in induced mice were comparable to literature values for patients. We administered methadone, a CNS-acting, P-glycoprotein substrate, to control and rifampin-induced transgenic mice and measured the drug's antinociceptive effect. In rifampin-induced mice, the methadone effect was reduced by about 70% even though plasma methadone levels were similar to those found in transgenic controls not exposed to rifampin. Thus, hPXR activation *in vivo* increased P-glycoprotein activity and tightened the blood-brain barrier to methadone, reducing the drug's CNS efficacy. This is the first demonstration of the ability of blood-brain barrier PXR to alter the efficacy of a CNS-acting drug.

INTRODUCTION

The blood-brain barrier, which resides within brain capillaries, is the primary determinant of drug entry into the CNS (Begley, 2003; Begley, 2004b). Barrier effectiveness reflects both the low permeability of tight junctions between capillary endothelial cells and the high expression of multispecific, ATP-driven drug-efflux pumps on the luminal membrane of those cells (Begley, 2004a). Of these transporters, P-glycoprotein presents the most formidable obstacle to CNS pharmacotherapy. Knocking out P-glycoprotein or reducing its transport function (activity) substantially increases brain levels of chemotherapeutics, HIV protease inhibitors, anticonvulsants, antipsychotics and glucocorticoids, raising the possibility of devising maneuvers to modulate P-glycoprotein function and thus selectively improve drug access to the CNS (Schinkel et al., 1994; Schinkel et al., 1996). Indeed, this potential has been realized in recent animal studies with the chemotherapeutic, taxol, a drug that is normally ineffective against brain tumors. Pre-treating mice with a specific P-glycoprotein inhibitor increased brain levels of administered taxol and reduced the mass of an intracerebrally implanted human glioblastoma by 90% (Fellner et al., 2002).

The converse of this argument is that increased P-glycoprotein activity should selectively close the blood-brain barrier, impeding therapy with P-glycoprotein substrates that normally cross the barrier in sufficient quantity to produce beneficial CNS effects, e.g., methadone, morphine, dexamethasone and some antiepileptics. This has been observed in animals chronically exposed to certain P-glycoprotein substrates (Fromm et al., 1997; Lotsch et al., 2002), but the mechanism underlying the increase in transporter activity has not been identified. We recently detected expression of the ligand-activated, pregnane X receptor (PXR) in isolated rat brain capillaries (Bauer et al., 2004). Previous studies in liver and gut had shown that

xenobiotics, e.g., steroids, statins, chemotherapeutics and endocrine disruptors, acting through PXR transcriptionally upregulate P-glycoprotein expression in those tissues (Dussault and Forman, 2002). We found similar upregulation of transporter expression and parallel increases in P-glycoprotein activity in isolated rat brain capillaries exposed to the xenobiotics, PCN and dexamethasone, both ligands for rodent PXR (Bauer et al., 2004). We also found substantially increased expression and activity in capillaries isolated from rats dosed with PCN and dexamethasone. These results defined a cause and effect relationship between activation of brain capillary PXR by xenobiotics and increased P-glycoprotein activity. They provide a context within which to examine the pharmacological consequences of activating PXR and increasing P-glycoprotein expression at the blood-brain barrier.

For the experiments reported here, we used a transgenic mouse expressing human PXR (hPXR) rather than mouse PXR (mPXR) (Xie et al., 2000). This choice of animal model is crucial because the ligand specificity of PXR varies substantially with species (Xie and Evans, 2002). The present results for transgenic mice expressing hPXR show increased P-glycoprotein expression and transport activity in isolated brain capillaries exposed to two high affinity hPXR ligands, rifampin, an antibiotic, and hyperforin, a constituent of the herbal remedy, St. John's wort. They also show increased transporter expression and activity in brain capillaries isolated from transgenic mice dosed with rifampin. To determine the consequences of hPXR induction of P-glycoprotein activity, we administered methadone, a CNS-acting P-glycoprotein substrate that normally produces a substantial antinociceptive effect, to control and rifampin-induced transgenic mice. In mice pretreated with rifampin, the methadone antinociceptive effect was substantially reduced, even though plasma methadone levels were unchanged. Thus, hPXR

activation increased P-glycoprotein expression and tightened the blood-brain barrier, reducing the efficacy of methadone.

MATERIALS and METHODS

Chemicals

Rifampin was purchased from Spectrum Chemical & Laboratory Products (Gardena, CA). Pregnenolone-16 α -carbonitrile (PCN), hyperforin, and methadone were purchased from Sigma (St. Louis, MO). [N- ϵ (4-nitrobenzofurazan-7-yl)-D-Lys⁸]-cyclosporine A (NBD-CSA) was custom-synthesized by Novartis (Basel, CH) (Schramm et al., 1995). PSC833 was a kind gift from Novartis (Basel, CH). All other chemicals were of analytical grade and were obtained from commercial sources.

Animals

Male CB6F1 wild-type mice (Charles River Laboratories, Wilmington, MA), CB6F1 hPXR transgenic mice (25-35g) and male CF-1 [*mdr1a*(+/+) and *mdr1a*(-/-)] mice (30-40 g; Charles River Laboratories) were used. CB6F1 hPXR (Xie et al., 2000) mice were a generous gift from Dr. Wen Xie (University of Pittsburgh, PA). Animal housing and dosing protocols were approved by the Institutional Animal Care and Use Committee of the University of North Carolina and were in accordance with NIH guidelines.

For in vitro studies, mice were decapitated and brains taken immediately for capillary isolation. For in vivo studies, mice were dosed daily for 1-3 days with 50 mg/kg rifampin in 0.1% agarose by oral gavage (4 μ l 0.1% agarose/g, 12.5 μ g/ μ l 0.1% agarose; agarose at 37° C to keep it liquid); controls received agarose alone. Twenty-four hours after the last dose, mice were decapitated and brains were taken immediately for capillary isolation. Intestinal mucosa and livers were snap-frozen in liquid nitrogen and stored at -80°C until use.

Capillary Isolation

Mouse brain capillaries were isolated as described previously (Bauer et al., 2004; Hartz et al., 2004) with slight modifications. Mice were decapitated and brains were immediately put in ice-cold DPBS buffer (2.7 mM KCl, 1.46 mM KH₂PO₄, 136.9 mM NaCl, 8.1 mM Na₂HPO₄, supplemented with 5 mM D-glucose and 1 mM Na-pyruvate, pH 7.4). Brains were homogenized in buffer, the homogenate was mixed with Ficoll[®] (final concentration 15%, Sigma, St. Louis, MO) and centrifuged at 5,800g for 10 min at 4°C. The resulting pellet was suspended in DPBS containing 1% BSA and passed over a glass bead column. Capillaries adhering to the glass beads were collected by gentle agitation in DPBS (1% BSA). Capillaries were washed three times in BSA-free DPBS and then used for experiments. For in vitro dosing studies, freshly isolated capillaries were first incubated in BSA-free DPBS buffer with PCN, rifampin or hyperforin for 6 hours at room temperature and then used for transport assays and immunostaining experiments. Capillaries from mice dosed in vivo were used immediately after isolation.

P-glycoprotein-Mediated Transport

Details of the transport assay are presented in (Bauer et al., 2004; Hartz et al., 2004). Briefly, isolated brain capillaries were incubated for 1 hour at room temperature in BSA-free DPBS buffer containing 2 μM NBD-CSA, a fluorescent P-glycoprotein substrate. Confocal images of 10-15 capillaries were acquired (Zeiss 410 meta laser scanning confocal microscope, 40× water immersion objective, NA=1.2, 488 nm line of argon laser) and luminal fluorescence intensity was measured from stored images using Scion Image software as described previously (Miller et al., 2000).

P-glycoprotein Immunostaining

Isolated mouse brain capillaries were fixed for 5-10 min with 3% paraformaldehyde/0.25% glutaraldehyde at room temperature. After washing with DPBS,

capillaries were permeabilized for 15 minutes with 0.5% (v/v) Triton X-100, and washed with DPBS containing 1% BSA. Then, capillaries were incubated for 1 hour at 37°C with a 1:100 dilution (1 µg/ml) of polyclonal rabbit antibody mdr ab-1 (Oncogene Research Products, Cambridge, MA). Capillaries were washed and incubated with Alexa Fluor[®] 488-conjugated anti-rabbit secondary IgG (1:1,000; Molecular Probes, OR) for 1 hour at 37°C. Nuclei were counterstained with 2.5 µg/ml propidium iodide. Negative controls for each treatment were processed without primary antibody and these showed only background fluorescence.

Immunofluorescence was visualized by confocal microscopy (Zeiss LSM 510 Meta Laser Scanning Confocal Microscope). For quantitating P-glycoprotein immunofluorescence, confocal images of 10-20 capillaries per treatment were acquired. Luminal membrane P-glycoprotein immunofluorescence for each capillary was measured using ImageJ software (version 1.29). A 10x10 grid was superimposed on each image and measurements of capillary luminal plasma membrane were taken between intersecting grid lines. The fluorescence intensity for each capillary was the mean of all measurements.

Western Blotting

Brain capillaries, intestinal mucosa and livers were homogenized in lysis buffer containing Complete[™] protease inhibitor cocktail (Roche, Mannheim, FRG). Homogenized samples were centrifuged at 10,000g for 15 min, denucleated supernatants were centrifuged at 100,000g for 90 min. Pellets (crude plasma membranes) were suspended in buffer containing protease inhibitor cocktail and protein concentrations were determined. Western blots were performed using the Invitrogen (Carlsbad, CA) NuPage[™] electrophoresis and blotting system. After blocking, membranes were incubated overnight with monoclonal mouse C219 primary antibody to P-glycoprotein (1:100, Signet, Dedham, MA). Membranes were washed and

incubated with the anti-mouse horseradish peroxidase-conjugated ImmunoPure[®] secondary antibody (1:15,000, Pierce, Rockford, IL) for 1 h. P-glycoprotein was detected using SuperSignal[®] West Pico Chemoluminescent Substrate (Pierce, Rockford, IL). Bands were visualized with a BioRad Gel Doc 2000[™] gel documentation system (BioRad, Hercules, CA).

Total RNA Isolation and RT-PCR

Total RNA from brain, intestine and liver of wild-type and hPXR transgenic mice was isolated using TRIzol[®] reagent (Invitrogen, Carlsbad, CA) and purified using the RNeasy Mini kit (Qiagen, Valencia, CA). Reverse transcription of total RNA was performed using the GeneAmp kit according to the manufacturer's protocol (Applied Biosystems, Foster City, CA). RT products were used for PCR of mPXR (GenBank No. NM_010936, forward: 5'-CTCTGCCTTGGAAGAGCCCATCAAC-3', bases 392-416; reverse: 5'-GGTTTGCATCTGAGCGTCCATCAGC-3', bases 785-809; 418 bp amplicon), hPXR (GenBank No. AY091855, forward: 5'-GTCTGTTTCCTGGAAAGCCCAGTGTC-3', bases 645-669; reverse: 5'-TCATCATCCGCTGCTCCTCTGTCAG-3', bases 1009-1033; 389 bp amplicon), and mGAPDH (GenBank No. BC083149, forward: 5'-GTATGTCGTGGAGTCTACTGGTGTC-3', bases 309-333; reverse: 5'-GGTGCAGGATGCATTGCTGACAATC-3', bases 465-489; 181 bp amplicon). PCR for brain, intestine and liver mPXR, hPXR and GAPDH was run 35 cycles; PCR for brain capillary GAPDH was run 35 cycles; PCR for brain capillary mPXR and hPXR was run 45 cycles. All primers were screened for specificity by using the PubMed BLAST database. Primers were custom-synthesized by Operon (Huntsville, AL) or MWG (High Point, NC), respectively. PCR products were separated by agarose gel electrophoresis.

Rifampin Dosing and Plasma Levels

To determine an appropriate rifampin dose for P-glycoprotein induction, unbound rifampin peak plasma concentration (free C_{\max}) following a single oral dose and unbound rifampin average plasma concentration (free C_{average}) at steady state following multiple, single daily doses were determined. In initial experiments, hPXR transgenic mice ($n = 20$) received a single dose of 50 mg/kg rifampin in 0.1% agarose by oral gavage. Blood samples (50 μ l) were collected by tail nick in heparinized capillary tubes over the next 36 hours. Blood was centrifuged (3,000g for 10 min) and plasma was obtained. Rifampin plasma concentrations were determined by HPLC-MS (Yang et al., 2003). Total rifampin peak plasma concentration (total C_{\max}) was obtained directly from the observed concentration time data profile. Free rifampin peak plasma concentration (free C_{\max}) was calculated from equation (1):

$$\text{free } C_{\max} = (1 - 0.88) * \text{total } C_{\max} \quad (1)$$

where 0.88 is bound fraction of rifampin in mouse plasma as determined by us. The area under the concentration time curve from time zero to infinity ($AUC_{0-\infty}$, i.e., total rifampin exposure) was calculated using the trapezoidal method with WinNonlin Software 4.1 (Pharsight, Mountain View, CA). Average total plasma rifampin concentration (C_{average}) at steady state following three single daily doses was calculated using equation (2):

$$C_{\text{average}} = AUC_{0-24} / \tau \quad (2)$$

where τ is the dosing interval (24 hours) and AUC_{0-24} at steady state following multiple dose is equal to $AUC_{0-\infty}$ following a single dose. The average free rifampin plasma concentration was then calculated from equation (1).

Methadone Antinociceptive Response

An electrical stimulation vocalization assay (ESV; threshold voltage to elicit vocalization of mice in response to an electrical stimulus) was used to determine the methadone-associated

antinociceptive response (Paalzow, 1969a; Paalzow, 1969b). Electrodes were inserted subdermally in the tails of ketamine-xylazine (85 and 0.3 mg/kg, respectively) anesthetized control and rifampin-treated hPXR transgenic mice (50 mg/kg rifampin daily for 3 days by oral gavage, 5 mice per group). Twenty-four hours after the last dose, baseline ESV was determined for each mouse. Subsequently, methadone was administered (3 mg/kg s.c.) and tests were repeated at multiple times for up to 8 h. For each mouse at each time, the antinociceptive effect (% ANE) was calculated as percent increase in voltage threshold using equation (3):

$$\% ANE = \left(\frac{ESV_{Methadone} - ESV_{Baseline}}{ESV_{Baseline}} \right) \times 100 \quad (3)$$

where $ESV_{Methadone}$ is the voltage causing vocalization after methadone administration and $ESV_{Baseline}$ is the voltage causing vocalization without methadone administration. The area under the antinociceptive effect vs. time curve (0-480 min) was determined using the trapezoidal method.

Methadone Plasma and Brain Disposition

hPXR transgenic mice in both vehicle- and rifampin-treated groups received a 3 mg/kg subcutaneous (s.c.) dose of methadone dissolved in saline. Blood samples were collected in heparinized capillary tubes by tail nick before methadone administration and at various times thereafter. Three to four mice were sampled at each time point. Blood was centrifuged at 2,000 g for 15 min and plasma was obtained. Samples were immediately frozen and stored at -80°C for later analysis by HPLC-MS.

In a separate series of experiments, male CF-1 [*mdr1a*(+/+) and *mdr1a*(-/-)] mice (30-40 g; Charles River Laboratories, Inc. Wilmington, MA) were used to establish a relationship

between antinociceptive effect and brain tissue concentration of methadone. Briefly, in a dose-response experiment, mice received a single subcutaneous injection of methadone (0.6-6 mg/kg for *mdr1a*(+/+) mice and 0.2-1.5 mg/kg for *mdr1a*(-/-) mice). Antinociception was evaluated at 30 min post-dose; animals were sacrificed for collection of brain tissue and serum (from trunk blood). Additional animals were utilized to assess antinociception and methadone concentrations at various times after methadone administration. *Mdr1a*(+/+) and *mdr1a*(-/-) mice received a single subcutaneous dose of methadone (4 or 1 mg/kg, respectively), and antinociception, brain tissue methadone, and serum methadone concentrations were determined at selected time intervals through 3 h post-dose. To construct the effect vs. concentration relationship, antinociception was expressed as percent of maximum, and a sigmoidal E_{\max} model was fit to the effect vs. concentration data.

For methadone analysis, 25 μ l of plasma or brain homogenate was mixed with 100 μ l methanol containing an internal standard (loperamide 50 ng/ml) to precipitate protein. The mixture was vortexed for 2 min, centrifuged at 16,000g for 10 min, and 5 μ l of supernatant was taken for analysis using an Agilent 1100 series HPLC-MS (Wilmington, DE) system. The system consisted of a single-quadrupole mass spectrometer (G1946D), a capillary pump (G1376A), a micro vacuum degasser (G1379A), and a microALS autosampler (G1389A). The supernatant was injected onto a Luna C₈ reverse phase column 30 x 2 mm (Torrance, CA) at room temperature. Analytes were eluted with an isocratic mobile phase containing 60% methanol and 40% 10mM ammonium acetate (pH 6.8) at a flow rate of 400 μ l/min and a retention time of 0.5 and 0.6 min, respectively. The mass spectrometer was operated in electrospray ionization (ESI) positive mode. Analysis was carried out using selected ion monitoring (SIM) for specific *m/z* 309.2 (methadone) and *m/z* 477.2 (loperamide); sensitivity of quantitation was 0.01 ng/ml. The

calibration curve was linear in the range of 0.1 to 100 ng/ml. The mean of intra-day and inter-day precision was 7.2 – 3.1 % (% CV) and 8.4 – 2.2% (% CV), respectively and the recovery ratio was > 98.7%.

Statistical Analysis

Observations are generally reported as mean \pm standard error. One or two-tail unpaired Student's t-test was used to evaluate differences between controls and treatment groups; differences were considered to be statistically significant when $P < 0.05$.

RESULTS

PXR exhibits distinct species differences in ligand specificity (Xie and Evans, 2002). For example, the St. John's Wort constituent, hyperforin, and the antibiotic, rifampin, are hPXR ligands but not rodent PXR ligands. On the other hand, pregnenolone-16 α -carbonitrile (PCN) is a high-affinity ligand for rodent PXR, but does not activate hPXR. To further understanding of the role of hPXR in metabolism based drug-drug interactions, Xie et al. generated a transgenic, 'humanized' mouse expressing hPXR, but lacking mPXR (Xie et al., 2000). Using Northern blot analysis they found that hPXR expression was liver-specific, which was expected due to the albumin-based vector used for transfection. Xie et al. further demonstrated that these mice responded to hPXR ligands, e.g., rifampin, by upregulating hepatic Cyp3A11 expression (Xie et al., 2000). As a consequence, rifampin-induced mice exhibited reduced sensitivity to two toxicants that are metabolized by hepatic Cyp3A11, tribromoethanol and zoxazolamine. Using a more sensitive assay for gene expression, RT-PCR, we have confirmed some of the initial findings of Xie et al. (Xie et al., 2000). As shown in Figure 1A, livers from transgenic mice expressed hPXR but not mPXR; in livers from wild-type mice, the reverse was true. However, in transgenic mice we detected hPXR expression in intestine, whole brain homogenate (Figure 1A) and isolated brain capillaries (Figure 1B) as well as liver; no mPXR expression was detected in any tissue. Thus, RT-PCR showed that hPXR expression in these transgenic mice was not liver-specific as had been originally reported. At present, we have no explanation for this discrepancy other than the high sensitivity of RT-PCR. This technique previously allowed us to detect PXR expression in rat brain homogenates (Bauer et al., 2004) when none had been detected by other laboratories using Northern blots (Jones et al., 2000; Kliewer et al., 1998; Zhang et al., 1999).

We took advantage of this expression pattern to determine the effects of ligands for mPXR (PCN) and hPXR (rifampin and hyperforin) on P-glycoprotein expression and activity in isolated brain capillaries from wild-type and hPXR transgenic mice. When we exposed freshly isolated capillaries from wild-type mice to 5 μ M PCN for 6 hours, luminal membrane P-glycoprotein immunofluorescence increased significantly (Figure 2A). Quantitation of luminal membrane P-glycoprotein immunofluorescence revealed a $53 \pm 6\%$ increase with PCN ($P < 0.001$, Figure 2C). Neither hyperforin nor rifampin increased P-glycoprotein immunofluorescence. This is the same pattern of induction seen in our previous study using rat brain capillaries (Bauer et al., 2004). When we repeated these in vitro dosing experiments with capillaries isolated from hPXR transgenic mice, hyperforin and rifampin increased luminal membrane P-glycoprotein immunofluorescence, but PCN did not (Figures 2B and 2D).

We have developed a method to measure P-glycoprotein transport activity in living, intact, isolated brain capillaries. It is based on measuring steady state, concentrative accumulation of the fluorescent, P-glycoprotein substrate, NBD-cyclosporin A (NBD-CSA) in capillary lumens using confocal microscopy and quantitative image analysis (Bauer et al., 2004; Hartz et al., 2004; Miller et al., 2000). Figure 3A shows brain capillaries from wild-type mice that were incubated with 2 μ M NBD-CSA for 60 min. Relative to bath, NBD-CSA fluorescence intensity was high in capillary lumens (Figure 3A, left). In agreement with previous studies using capillaries from rat (Bauer et al., 2004; Fellner et al., 2002; Hartz et al., 2004), the P-glycoprotein-specific inhibitor, PSC833, reduced luminal NBD-CSA accumulation (Figure 3A, right). Inhibition was maximal with 5 μ M PSC833, resulting in about a 50% reduction; exposing capillaries to 1 mM NaCN produced the same level of transport inhibition (not shown). Thus, the PSC833-sensitive component of NBD-CSA accumulation in the lumens of isolated mouse brain

capillaries represents active, P-glycoprotein-specific transport. Remaining luminal fluorescence (PSC833-insensitive component) probably represents simple diffusion and unspecific binding of NBD-CSA to capillary tissue (Bauer et al., 2004; Hartz et al., 2004). In the present experiments the PSC833-insensitive component averaged 52-54 fluorescence units and was not altered when capillaries were exposed to PXR ligands or when animals were dosed with rifampin (not shown).

Figure 3B shows PSC833-sensitive, luminal NBD-CSA fluorescence in capillaries from wild-type mice that were exposed for 6 hours to PCN, hyperforin or rifampin. Consistent with the quantitative immunostaining results and the ligand specificity of mPXR, PCN doubled luminal NBD-CSA accumulation, but hyperforin and rifampin had no significant effects. In contrast, when this experiment was carried out with capillaries from hPXR transgenic mice, both hyperforin and rifampin increased P-glycoprotein-mediated transport in a concentration-dependent manner, but PCN, was without effect (Figure 3C). The observed increases in P-glycoprotein expression and activity in response to rifampin and hyperforin are consistent with the expression of functional hPXR in brain capillaries.

To determine whether in vivo exposure to an hPXR ligand increased P-glycoprotein expression and transport activity, we dosed hPXR transgenic mice daily for 3 days by oral gavage with 50 mg/kg rifampin. We chose this dose level based on preliminary experiments in which we measured plasma rifampin levels in dosed mice and compared them to literature values for patients receiving a therapeutic dose of the drug. In mice, after a single oral dose of 50 mg/kg rifampin, maximal total plasma levels averaged 7.72 $\mu\text{g/ml}$. Of this 88% was bound to plasma proteins, giving a free concentration of 0.93 $\mu\text{g/ml}$. Corresponding values for patients receiving a single oral dose of 6.4 mg/kg rifampin are 5.41 and 1.08 $\mu\text{g/ml}$ (80% plasma protein binding) (Agrawal et al., 2002). Similarly, predicted free C_{average} at steady state following multiple doses

is also the same for human and mouse, 0.34 and 0.35 $\mu\text{g/ml}$, respectively (see Methods). Thus, dosing mice with 50 mg/kg rifampin daily resulted in peak plasma levels of free drug similar to those seen in patients taking single, daily 6.4 mg/kg oral doses (448 mg dose for 70 kg patient).

Figures 4A and 4B show Western blots of membranes isolated from intestine, liver and brain capillaries of control and rifampin-dosed hPXR transgenic mice. Rifampin-dosing increased P-glycoprotein immunoreactivity in all three tissues. Consistent with this, luminal membrane P-glycoprotein immunofluorescence in capillaries from rifampin-dosed hPXR transgenic mice was significantly higher than in capillaries from control hPXR mice (Figures 4C and 4D). In addition, P-glycoprotein activity (measured as PSC833-sensitive luminal NBD-CSA accumulation) in brain capillaries from rifampin-dosed mice was more than double that found in capillaries from controls (Figure 4E).

Having demonstrated increased P-glycoprotein expression and activity in brain capillaries from transgenic mice after dosing with hPXR ligands, we used these mice to determine the extent to which hPXR activation would alter the efficacy of a drug that is both CNS-active and a P-glycoprotein substrate. Several classes of CNS-acting drugs include members that are P-glycoprotein substrates, e.g., antiepileptics, analgesics and anti-inflammatory steroids (Balayssac et al., 2005). Clearly, to act these must enter the brain to some extent. One consequence of increased brain capillary expression of P-glycoprotein should be reduced brain penetration of these drugs and thus reduced CNS efficacy. To test this supposition, we assayed the antinociceptive effect of methadone in hPXR transgenic mice dosed orally for 3 days with 50 mg/kg rifampin and in vehicle-dosed transgenic mice (controls). Methadone is one P-glycoprotein substrate that enters the CNS in sufficient quantity to have an easily measurable CNS effect (analgesia). This antinociceptive effect is substantially enhanced in P-glycoprotein

knock-out mice (Dagenais et al., 2004; Zong and Pollack, 2003). The assay we used measured the tolerance of mice to an electrical stimulus before and after administration of 3 mg/kg subcutaneous methadone (antinociceptive effect; see Methods). In agreement with previous studies (Dagenais et al., 2004), methadone substantially increased tolerance in control mice. Thirty-five min after methadone dosing, mice tolerated a stimulus almost 3 times greater ($271.2 \pm 27.7\%$) than they could in trials without methadone (response set at 100%; Figure 5A). In transgenic mice pretreated with rifampin, methadone still had an antinociceptive effect, but this effect was substantially blunted. Thirty-five min after dosing, rifampin-treated mice could tolerate a stimulus only 1.5 times greater ($151.5 \pm 32.5\%$) than without methadone. Thus, rifampin pretreatment reduced methadone's antinociceptive effect to about 30% of that found in mice not given rifampin. In addition, the overall magnitude of antinociceptive effect as indicated by the area under the time-effect curve (0-480 min) was significantly lower in mice pretreated with rifampin ($133 \pm 17\% \times \text{min}$), than in controls ($422 \pm 65\% \times \text{min}$; $P < 0.05$).

Since measurements of mean plasma methadone levels over the entire time course of the experiment showed no significant differences between control and rifampin-dosed mice (Figure 5B), the effect of rifampin pretreatment on methadone efficacy appeared to have resulted from reduced methadone access to CNS sites of action rather than from increased methadone excretion or metabolism in peripheral tissues. To define the relationship between antinociceptive effect and brain tissue concentrations of methadone, additional experiments were performed in separate groups of mice. CF-1 mice [*mdr1a*(+/+) and *mdr1a*(-/-)] were used for this animal-intensive effort. Figure 6A shows dose response relationships for wild-type and *mdr1a*(-/-) mice. As one would expect, the curve for *mdr1a*(-/-) mice was shifted substantially to the left. Plots of brain vs serum methadone concentration were linear. It was clear from these plots that the slope

of the line for *mdr1a*(-/-) mice was substantially higher than for wild-type mice; equivalent plasma methadone concentrations produced roughly 6-fold higher brain concentrations in the *mdr1a*(-/-) mice. These results confirm previous studies on methadone effectiveness and brain levels in mice (Dagenais et al., 2004; Thompson et al., 2000). Figure 6C shows the relationship between antinociceptive effect and brain methadone concentration in these mice. Note that to observe the full response, different methadone dose ranges were used for wild-type (0.6-6 mg/kg) and *mdr1a*(-/-) (0.2-1.5 mg/kg) mice. Nevertheless, the data combined fit to a single sigmoidal E_{\max} model. The relationship between antinociceptive effect and brain methadone concentration is clearly the same for both wild-type and *mdr1a*(-/-) mice, i.e., it is independent of P-glycoprotein status. These results indicate that antinociception provides a reasonable surrogate for brain tissue concentrations of methadone in mice. Importantly, they argue that the decrease in antinociceptive effect seen in rifampin dosing experiments with hPXR transgenic mice was a result of decreased brain methadone accumulation.

DISCUSSION

Polypharmacy is a fact of life in the clinic. With it comes the potential for drug-drug interactions that alter dose-response relationships and thus can affect drug efficacy and safety. Such interactions can be direct, e.g., when two drugs compete for common sites of action, metabolism or transport, or indirect, e.g., when one drug alters the expression of genes that determine the action, metabolism or distribution of a second drug. The present results for a humanized, transgenic mouse provide an example of the latter. Using isolated brain capillaries, we demonstrated increased expression and transport activity of the drug efflux pump, P-glycoprotein, after exposure to the hPXR ligands, rifampin and hyperforin. Similar increases in P-glycoprotein expression and activity were found in capillaries from mice dosed orally with rifampin. Moreover, rifampin dosing substantially reduced the effectiveness of the CNS-acting drug and P-glycoprotein substrate, methadone, without changing plasma methadone levels. In these experiments plasma rifampin levels were similar to those measured in patients undergoing antibiotic therapy, suggesting that similar effects would be seen in patients exposed to therapeutic levels of rifampin.

In previous *in vitro* and *in vivo* experiments with the rodent-specific PXR ligand, PCN, we found maximal induction of P-glycoprotein expression and activity was about 2-fold in rat brain capillaries (Bauer et al., 2004). The present data for mouse indicates roughly the same extent of maximal induction *in vitro* in capillaries from wild-type (with PCN) and transgenic (with rifampin) animals. Thus, the extent to which activation of PXR increases P-glycoprotein expression in brain capillaries from rodents is consistent. In the present *in vivo* dosing experiment with transgenic mice, the dose of rifampin used was selected to give plasma levels that matched those found in patients. Although the increase in P-glycoprotein activity and

expression was comparable to that seen *in vitro*, it is not clear whether this dose produced a maximal effect *in vivo*. Certainly, these experiments with an animal model do not tell us with quantitative certainty the extent to which rifampin will induce P-glycoprotein expression in patients or how that change in transporter expression will translate into a pharmacodynamic effect. Taken together, these *in vitro* and *in vivo* experiments indicate that hPXR ligands can upregulate expression of a key element of the blood-brain barrier and produce a selective tightening of that barrier.

PXR-driven upregulation of P-glycoprotein at the blood-brain barrier (and peripheral tissues) has important clinical implications. The wide specificity limits of both P-glycoprotein (roughly half of commonly prescribed drugs) and hPXR (a growing list of metabolites, drugs and dietary constituents) argue that hPXR-based changes in selective barrier function should be widespread in the population. They are likely contributors to the difficulties encountered in chemotherapy of brain tumors, to the multidrug resistance seen in epileptics and to patient-to-patient variability in response to CNS-acting drugs (Loscher and Potschka, 2005a; Loscher and Potschka, 2005b). On the other hand, recognition of the important role that hPXR plays in determining the level of P-glycoprotein expression at the blood-brain barrier, and thus of barrier selective permeability, may be a first step to devising simple treatments that can be used to prevent or reverse selective barrier tightening, e.g., restrictions in diet or careful choice of prescribed drugs. Clearly, the extent to which individual hPXR ligands will alter blood-brain barrier transport function in patients will depend on exposure levels, ligand affinity for the receptor and ligand pharmacokinetics.

REFERENCES

- Agrawal S, Singh I, Kaur KJ, Bhade SR, Kaul CL and Panchagnula R (2002) Bioequivalence assessment of rifampicin, isoniazid and pyrazinamide in a fixed dose combination of rifampicin, isoniazid, pyrazinamide and ethambutol vs. separate formulations. *Int J Clin Pharmacol Ther* **40**(10):474-481.
- Balayssac D, Authier N, Cayre A and Coudore F (2005) Does inhibition of P-glycoprotein lead to drug-drug interactions? *Toxicol Lett* **156**(3):319-329.
- Bauer B, Hartz AM, Fricker G and Miller DS (2004) Pregnane x receptor up-regulation of p-glycoprotein expression and transport function at the blood-brain barrier. *Mol Pharmacol* **66**(3):413-419.
- Begley DJ (2003) Understanding and circumventing the blood-brain barrier. *Acta Paediatr Suppl* **92**(443):83-91.
- Begley DJ (2004a) ABC transporters and the blood-brain barrier. *Curr Pharm Des* **10**(12):1295-1312.
- Begley DJ (2004b) Delivery of therapeutic agents to the central nervous system: the problems and the possibilities. *Pharmacol Ther* **104**(1):29-45.
- Dagenais C, Graff CL and Pollack GM (2004) Variable modulation of opioid brain uptake by P-glycoprotein in mice. *Biochem Pharmacol* **67**(2):269-276.
- Dussault I and Forman BM (2002) The nuclear receptor PXR: a master regulator of "homeland" defense. *Crit Rev Eukaryot Gene Expr* **12**(1):53-64.

- Fellner S, Bauer B, Miller DS, Schaffrik M, Fankhanel M, Spruss T, Bernhardt G, Graeff C, Farber L, Gschaidmeier H, Buschauer A and Fricker G (2002) Transport of paclitaxel (Taxol) across the blood-brain barrier in vitro and in vivo. *J Clin Invest* **110**(9):1309-1318.
- Fromm MF, Eckhardt K, Li S, Schanzle G, Hofmann U, Mikus G and Eichelbaum M (1997) Loss of analgesic effect of morphine due to coadministration of rifampin. *Pain* **72**(1-2):261-267.
- Hartz AM, Bauer B, Fricker G and Miller DS (2004) Rapid regulation of p-glycoprotein at the blood-brain barrier by endothelin-1. *Mol Pharmacol* **66**(3):387-394.
- Jones SA, Moore LB, Shenk JL, Wisely GB, Hamilton GA, McKee DD, Tomkinson NC, LeCluyse EL, Lambert MH, Willson TM, Kliewer SA and Moore JT (2000) The pregnane X receptor: a promiscuous xenobiotic receptor that has diverged during evolution. *Mol Endocrinol* **14**(1):27-39.
- Kliewer SA, Moore JT, Wade L, Staudinger JL, Watson MA, Jones SA, McKee DD, Oliver BB, Willson TM, Zetterstrom RH, Perlmann T and Lehmann JM (1998) An orphan nuclear receptor activated by pregnanes defines a novel steroid signaling pathway. *Cell* **92**(1):73-82.
- Loscher W and Potschka H (2005a) Drug resistance in brain diseases and the role of drug efflux transporters. *Nat Rev Neurosci* **6**(8):591-602.
- Loscher W and Potschka H (2005b) Role of drug efflux transporters in the brain for drug disposition and treatment of brain diseases. *Prog Neurobiol* **76**(1):22-76.
- Lotsch J, Skarke C, Tegeder I and Geisslinger G (2002) Drug interactions with patient-controlled analgesia. *Clin Pharmacokinet* **41**(1):31-57.
- Miller DS, Nobmann SN, Gutmann H, Toeroek M, Drewe J and Fricker G (2000) Xenobiotic transport across isolated brain microvessels studied by confocal microscopy. *Mol Pharmacol* **58**(6):1357-1367.

- Paalzow L (1969a) An electrical method for estimation of analgesic activity in mice. I. Methodological investigations. *Acta Pharm Suec* **6**(2):193-206.
- Paalzow L (1969b) An electrical method for estimation of analgesic activity in mice. II. Application of the method in investigations of some analgesic drugs. *Acta Pharm Suec* **6**(2):207-226.
- Schinkel AH, Smit JJ, van Tellingen O, Beijnen JH, Wagenaar E, van Deemter L, Mol CA, van der Valk MA, Robanus-Maandag EC, te Riele HP and et al. (1994) Disruption of the mouse *mdr1a* P-glycoprotein gene leads to a deficiency in the blood-brain barrier and to increased sensitivity to drugs. *Cell* **77**(4):491-502.
- Schinkel AH, Wagenaar E, Mol CA and van Deemter L (1996) P-glycoprotein in the blood-brain barrier of mice influences the brain penetration and pharmacological activity of many drugs. *J Clin Invest* **97**(11):2517-2524.
- Schramm U, Fricker G, Wenger R and Miller DS (1995) P-glycoprotein-mediated secretion of a fluorescent cyclosporin analogue by teleost renal proximal tubules. *Am J Physiol* **268**(1 Pt 2):F46-52.
- Thompson SJ, Koszdin K and Bernards CM (2000) Opiate-induced analgesia is increased and prolonged in mice lacking P-glycoprotein. *Anesthesiology* **92**(5):1392-1399.
- Xie W, Barwick JL, Downes M, Blumberg B, Simon CM, Nelson MC, Neuschwander-Tetri BA, Brunt EM, Guzelian PS and Evans RM (2000) Humanized xenobiotic response in mice expressing nuclear receptor SXR. *Nature* **406**(6794):435-439.
- Xie W and Evans RM (2002) Pharmaceutical use of mouse models humanized for the xenobiotic receptor. *Drug Discov Today* **7**(9):509-515.

Yang X, Matheny CJ, White NR and Pollack GM (2003) Quantitative analysis of rifampin for evaluating pharmacokinetics and tissue distribution in mice. *Pharm Sci* **5**(4):4.

Zhang H, LeCulyse E, Liu L, Hu M, Matoney L, Zhu W and Yan B (1999) Rat pregnane X receptor: molecular cloning, tissue distribution, and xenobiotic regulation. *Arch Biochem Biophys* **368**(1):14-22.

Zong J and Pollack GM (2003) Modulation of P-glycoprotein transport activity in the mouse blood-brain barrier by rifampin. *J Pharmacol Exp Ther* **306**(2):556-562.

FOOTNOTES

This research was supported in part by the Intramural Research Program of the NIH, National Institute of Environmental Health Sciences and NIH grant GM61191 (to GMP).

Send reprint requests to:

Dr. David S. Miller
Laboratory of Pharmacology and Chemistry
National Institute of Environmental Health Sciences
P.O. Box 12233, MD F2-03
111 TW Alexander Drive
Research Triangle Park, NC 27709, USA
Phone: 919 541 3235
FAX: 919 541 5737
miller@niehs.nih.gov

FIGURE LEGENDS

Figure 1. PXR expression in mouse tissues. (A) RT-PCR of brain, intestine and liver from wild-type mice and hPXR transgenic mice. Top panel: Mouse PXR (mPXR, 418 bp amplicon, 35 cycles) is expressed in brain (B), intestine (I) and liver (L) of wild-type mice. Middle panel: Human PXR (hPXR, 389 bp amplicon, 35 cycles) is only expressed in hPXR transgenic mice. Bottom panel: GAPDH loading control (181 bp amplicon, 35 cycles, nc: negative control). (B) RT-PCR of brain capillaries from wild-type mice and hPXR transgenic mice. Top panel: mPXR is expressed in brain capillaries (BC) of wild-type mice (45 cycles). Middle panel: hPXR is only expressed in brain capillaries of hPXR transgenic mice (45 cycles). Bottom panel: GAPDH loading control (35 cycles, nc: negative control).

Figure 2. P-glycoprotein expression in brain capillaries after exposure to PXR ligands. (A) Representative images showing immunostaining of P-glycoprotein in isolated brain capillaries from wild-type mice. Exposing brain capillaries for 6 hours to PCN increased P-glycoprotein expression; rifampin (RIF) and hyperforin (HYP) had no effect (scale bar: 10 μ m). (B) Representative images showing immunostaining of P-glycoprotein in isolated brain capillaries from hPXR transgenic mice. 6 hour exposure of rifampin and hyperforin, but not PCN, increased P-glycoprotein expression in capillaries of hPXR transgenic mice (scale bar: 10 μ m). (C) Quantitation of luminal membrane P-glycoprotein immunofluorescence from capillaries of wild-type mice exposed to PCN, rifampin or hyperforin. (D) Concentration-dependent increase of luminal membrane P-glycoprotein immunofluorescence from isolated capillaries of hPXR transgenic mice exposed to rifampin or hyperforin; PCN had no effect. Each bar represents the

mean value (arbitrary fluorescence units, scale 0-255) of 15-20 capillaries from a single preparation (pooled tissue from 5 wild-type mice or 3 hPXR transgenic mice); variability is given by SE bars. Statistical comparison: ** significantly greater than control, $P < 0.01$, *** significantly greater than control, $P < 0.001$.

Figure 3. P-glycoprotein transport function in brain capillaries after exposure to PXR ligands.

(A) Left: Representative image showing steady state (60 min) NBD-CSA (2 μM) accumulation in two brain capillaries from wild-type mice. The arrows indicate red blood cells (dark) in the capillary lumen (bright). Right: Corresponding image for a capillary exposed to 5 μM PSC833. The arrow shows the capillary lumen with reduced fluorescence (scale bar: 10 μm). (B) Specific (PSC833-sensitive) NBD-CSA accumulation in the lumen of brain capillaries isolated from wild-type mice. 6 hour exposure to PCN increased luminal NBD-CSA; rifampin (RIF) and hyperforin (HYP) had no effect. (C) Concentration-dependent increase of specific NBD-CSA accumulation in the lumen of capillaries isolated from hPXR transgenic mice that were exposed to rifampin or hyperforin for 6 hours; PCN had no effect. Each bar represents the mean value (arbitrary fluorescence units, scale 0-255) of 10 capillaries from a single preparation (pooled tissue from 5 wild-type mice or 3 hPXR transgenic mice); variability is given by SE bars. *** significantly greater than control, $P < 0.001$.

Figure 4. Induction of P-glycoprotein expression and activity in hPXR transgenic mice after in vivo exposure to rifampin (50 mg/kg rifampin daily for three days by oral gavage). (A) P-glycoprotein Western blot from crude membrane fractions of intestine and liver of hPXR transgenic mice (Ctrl: Vehicle-dosed control animals; RIF: Rifampin-dosed animals, negative

control (-): brain homogenate, positive control (+): renal brush border membranes). (B) P-glycoprotein Western blot from plasma membranes of brain capillaries (BCM) isolated from vehicle-dosed controls (Ctrl) and rifampin-dosed (RIF) hPXR transgenic mice (negative control (-): brain homogenate, positive control (+): renal brush border membranes). (C) Representative images showing luminal membrane P-glycoprotein immunofluorescence in capillaries from vehicle-dosed and rifampin-dosed hPXR transgenic mice (scale bar: 10 μ m). (D) Quantitation of luminal membrane P-glycoprotein immunofluorescence from capillaries of hPXR transgenic mice. (E) Specific NBD-CSA accumulation (PSC833-sensitive) in the lumen of brain capillaries isolated from hPXR transgenic mice. Each bar represents the mean value (arbitrary fluorescence units, scale 0-255) of 10 capillaries from a single preparation (pooled tissue from 5 control hPXR transgenic mice or 6 rifampin-treated hPXR transgenic mice); variability is given by SE bars. Statistical comparison: *** significantly greater than control, $P < 0.001$.

Figure 5. Reduced efficacy of methadone in rifampin-dosed hPXR transgenic mice. Mice were dosed daily for 1-3 days with 50 mg/kg rifampin in 0.1% agarose by oral gavage (4 μ l 0.1% agarose/g, 12.5 μ g/ μ l 0.1% agarose); controls received agarose alone. Twenty-four hours after the last dose animals were tested to measure the methadone (3 mg/kg sc) antinociceptive effect as described in Methods. (B) Plasma methadone levels in transgenic mice as a function of time after dosing (3 mg/kg sc). Each point represents the mean value for 5 mice; variability is given by SE bars. Statistical comparison: * significantly less than controls, $P < 0.05$.

Figure 6. Relationship between antinociceptive effect and brain methadone concentration in *mdr1a*(+/+) (closed symbols) and *mdr1a*(-/-) (open symbols) CF-1 mice. (A) Dose response

curves for methadone antinociception. (B) Brain and serum methadone levels. Linear regression analysis indicated a good fit for the data from wild-type ($r^2 = 0.985$) and *mdr1a*(-/-) mice ($r^2 = 0.991$). The regression lines had similar intercepts but very different slopes (2.1 vs 11.7 ml/g for wild type and *mdr1a*(-/-) mice, respectively; $P < 0.01$). (C) Relationship between antinociceptive effect and brain tissue methadone concentration in *mdr1a*(+/+) (closed symbols) and *mdr1a*(-/-) (open symbols) at a fixed time (triangles) and at variable times (circles) post-methadone. Curve represents fit of a sigmoidal E_{\max} equation to the data ($r^2 = 0.728$); error bars were omitted for clarity.

Each point represents the mean value for 4-5 animals; when shown, error bars indicate SD.

Figure 1

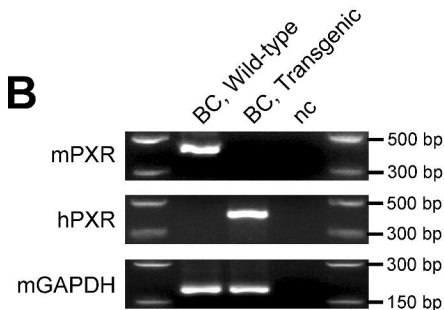
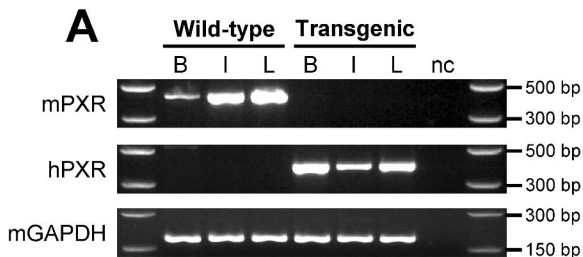


Figure 2

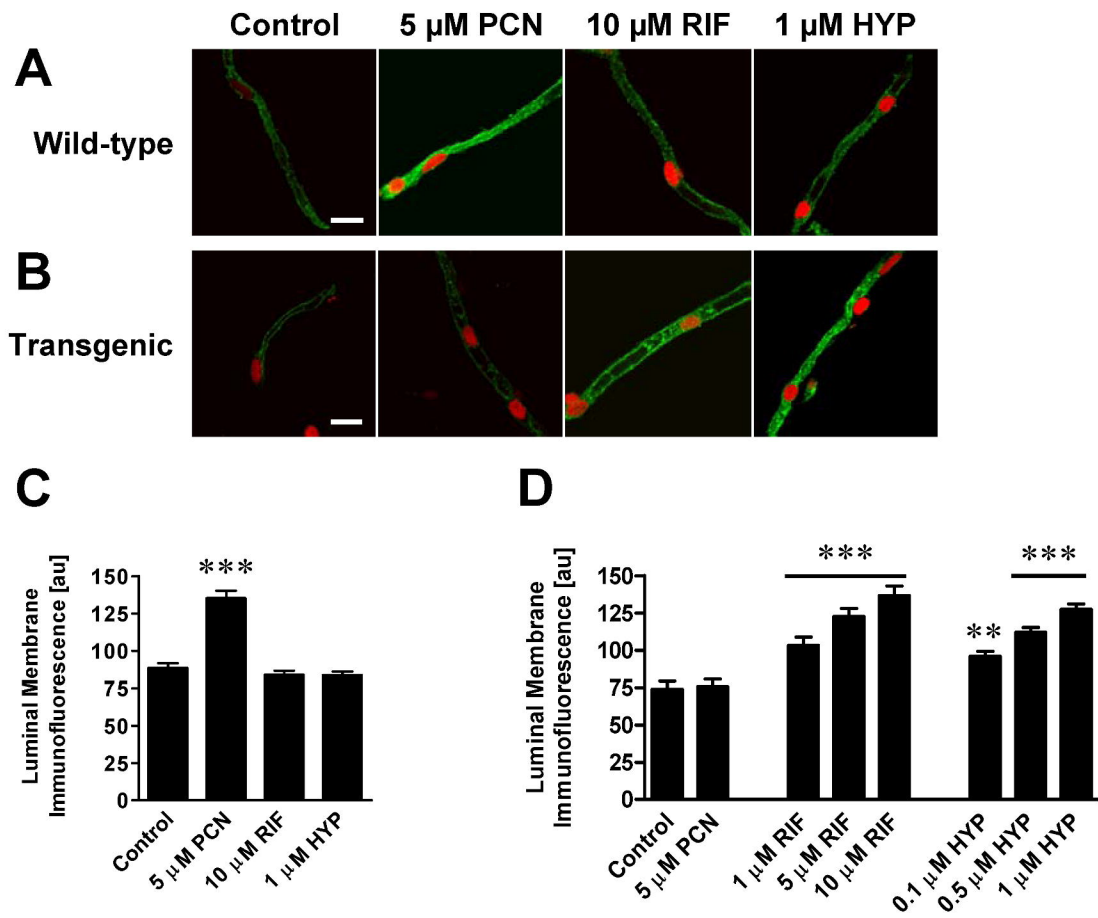


Figure 3

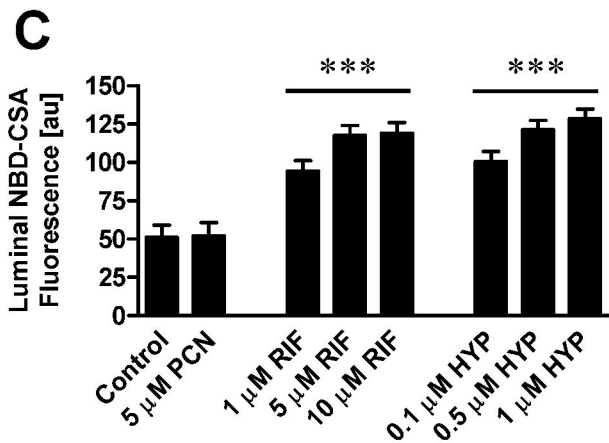
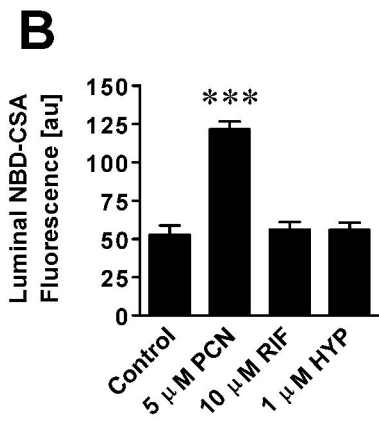
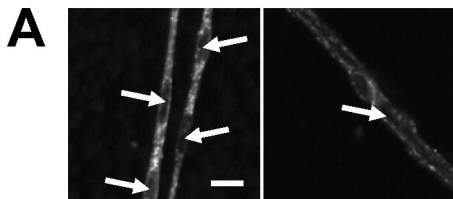


Figure 4

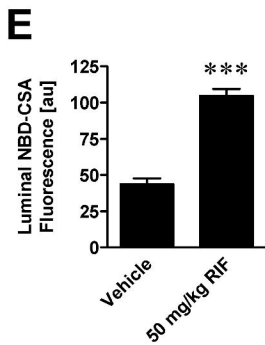
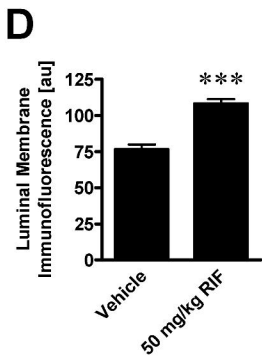
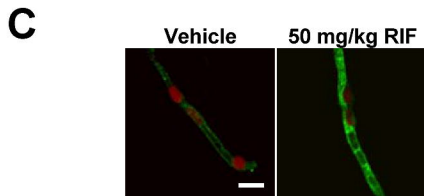
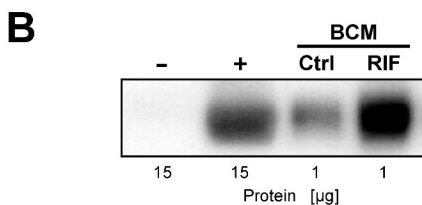
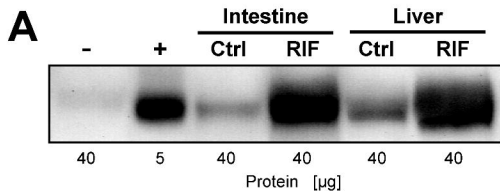


Figure 5

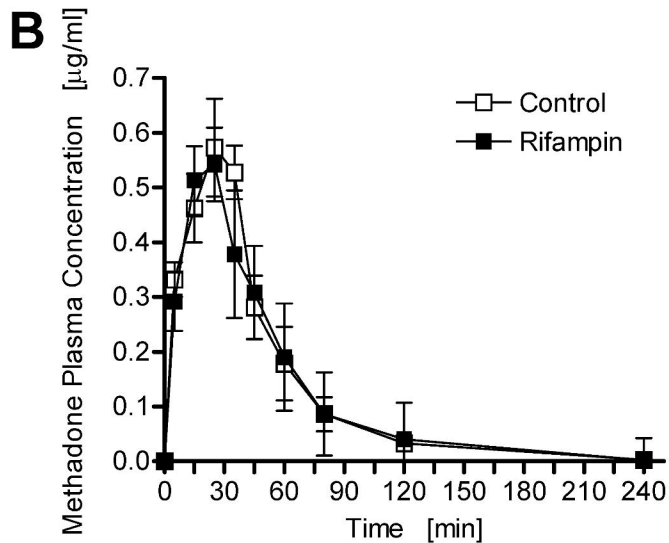
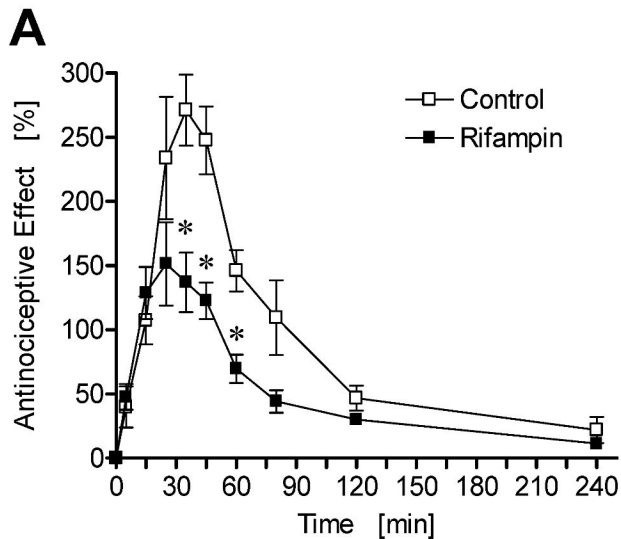


Figure 6

